

Contents lists available at ScienceDirect

International Journal of Mineral Processing

journal homepage: www.elsevier.com/locate/ijminpro



The effect of dissolution kinetics on flotation response of apatite with sodium oleate



Daniela Horta ^a, Marisa Bezerra de Mello Monte ^{b,*}, e Laurindo de Salles Leal Filho ^b

- ^a Mining Engineering Nucleus, Science and Technology Institute, Federal University of Alfenas (Unifal-MG), Poços de Caldas Campus, Brazil
- ^b Vale Institute of Technology (ITV Mining), Brazil

ARTICLE INFO

Article history: Received 18 March 2015 Received in revised form 22 September 2015 Accepted 9 December 2015 Available online 11 December 2015

Keywords: Flotation Apatite Sodium oleate Dissolution kinetics

ABSTRACT

Different flotation strategies are used to concentrate apatite from phosphate rock around the world. There is evidence that the flotation performance of apatite can be influenced by its dissolution kinetics. The objective of this study was to investigate the effect of dissolution kinetics parameters on the flotation response, with sodium oleate, of apatite samples from different origins and genesis. The samples were firstly purified and characterized by X-Ray Fluorescence (XRF) and the Rietveld method applied to X-Ray Diffraction data (RXD). Surface area, specific mass and porosity were also determined. Apatite dissolution experiments were carried out in an automated reactor. The apatite flotation responses were determined by means of microflotation experiments. Both types of tests were performed at pH 8 and 10. By means of exponential adjustment of the dissolution curves (accumulated amount of dissolved Ca²⁺ ions as a function of time) it was possible to calculate the maximum amount of dissolved Ca^{2+} ions (Ca^{2+}_{MAX}) and the kinetic constant (k). The initial dissolution rate (R_i) was determined by linear adjustment of the first minutes of reaction. It was observed that the initial dissolution rate, as well as the floatability, is greater at pH 8 than at pH 10. In addition, by comparing apatites from different origins it was found that the floatability increases with R_i and Ca^{2+}_{MAX} . The results indicate that the floatation performance is improved by the increase in the amount of Ca²⁺ ions that are available to interact with oleate molecules. This result supports the relevance of the surface precipitation mechanism governing the adsorption of oleate on the apatite surface.

 $\ensuremath{\text{@}}$ 2015 Published by Elsevier B.V.

Contents

1.		tion	
2.	Mater	s and methods	
	2.1.	patite samples	. 99
	2.2.	urification of apatites	. 99
	2.3.	haracterization	. 99
	2.4.	issolution experiments	100
	2.5.	lotation experiments	100
3.	Result		100
	3.1.	haracterization	100
	3.2.	vissolution	101
	3.3.	lotation response	102
	3.4.	viscussion	
4.	Conclu	ons	103
Ack	nowleds	nents	104

^{*} Corresponding author at: Vale Institute of Technology — ITV, Mining ITV, Avenida Juscelino Kubitschek, 31-Bauxita, Ouro Preto, Minas Gerais Cep: 35.400-000, Brazil. E-mail address: marisa.monte@itv.org (M.B. de Mello Monte).

 Table 1

 Flotation strategies applied to concentrate apatite from phosphate rock from different regions (Horta, 2013).

Genesis	Origin	Flotation route	Collector	Modifiers	рН
Sedimentary	China Brazil ^(a)	Reverse anionic	Fatty acid	H ₂ SO ₄ and H ₃ PO ₄	<5
	Mozambique and Brazil	Direct anionic	Alkyl sarcosinate ^(b) Alkyl sulfosuccinamate ^(c)	Starch NaOH	>10.5
Igneous	South Africa	Direct anionic	Fatty acid	Sodium silicate Gum arabic Nonylphenol	Natural (8-8.5)
Metamorphic	Brazil India	Reverse anionic Direct anionic	Fatty acid ^(d) Alkyl sarcosinates	H ₃ PO ₄ Starch	Acidic medium Basic medium

- ^a Irecê-BA.
- ^b Cajati-SP and Evate-Mozambique.
- ^c Tapira-MG.
- ^d Santa Quitéria-CE.

1. Introduction

Phosphate rock is a primary, nonrenewable, source of phosphorous (P) for inorganic fertilizers. The total demand must be met through the mining, beneficiation and chemical processing of apatite. More than 60% of the phosphate in the world is concentrated by froth flotation (Abouzeid, 2008; Sis and Chander, 2003a). The marketable phosphate concentrate must display contents of $P_2O_5 \leq 30\%$, $CaO/P_2O_5 < 1.6$,MgO/ $P_2O_5 < 0.022$ and MgO < 1% (Abouzeid, 2008; Lawendy and McClellan, 1993; Sis and Chander, 2003a, 2003b).

Apatite is the phosphorus (P) bearing mineral of phosphate deposits with different genesis: igneous (as in the carbonatite–alkaline complexes of Russia, Uganda, Brazil and South Africa); sedimentary (marine fosforites as in the north of Africa and Florida) and phosphates of organic accumulation (like the deposits of guano in Peru and Chile). Deposits from different genesis are characterized by the presence of several types of apatite: fluorapatite $(Ca_{10}(PO_4)_6F_2)$ in igneus rock; hidroxiapatite $(Ca_{10}(PO_4)_6(OH)_2)$ from biogenic origin; cloroapatite $(Ca_{10}(PO_4)_6Cl_2)$ in igneous rock, rocks affected by metasomatism with chlorine (Cl) and in some sedimentary environments; and Carbonate–fluorapatite $((Ca,Na,Mg)_{10}(PO_4,CO_3)_6(F,OH)_2)$ in sedimentary rock (Abouzeid et al., 1980; Toledo and Pereira, 2001).

Industrial practices and laboratory investigations have provided strong evidence that a flotation strategy, which is suitable to concentrate a specific phosphate ore, can completely fail to concentrate others. This fact is evidenced in Table 1, which shows that for some ores it is more worthwhile to accomplish direct flotation of apatite. Conversely, for other ores, it is more effective to conduct reverse flotation of carbonates (Abdel-Khalek, 2000; Assis et al., 1985; Leal Filho et al., 2010; Pugh and Stenius, 1985; Zheng et al., 2006).

Variances in mineralogical composition and P_2O_5 content are not sufficient to explain the dissimilar flotation response of phosphate ores from different origins (Table 1). Several works from 1985 to 1990 alerted to the influence of the intrinsic characteristics of minerals that compose the ore on the interaction between minerals and flotation reagents. Chemical heterogeneity, surface texture, crystallinity and dissolution degree are examples of intrinsic characteristics (Assis et al., 1987; Horta, 2013; Leal Filho, 1991; Silva et al., 1985).

In addition, the flotation success depends on the range of chemical reagents added to the system in order to control the surface characteristics of the minerals, determining the selectivity degree. Different types of reagents are used in the flotation of phosphate ores, such as collectors, depressants, and auxiliary reagents. Long chain anionic collectors such as fatty acids and alkyl sarcosinates, sulfossuccinates and sulfossuccinamates have been used for Ca-bearing minerals as observed in Table 1 (Hanna and Somasundaran, 1976; Leal Filho et al., 2010; Snow and Zhang, 2006; Yehia et al., 1993).

Sodium oleate (fatty acid) is the collector used in most of the works in the literature (Amankonah et al., 1985; Finkelstein, 1989; Hanna and Somasundaran, 1976; Lu et al., 1998; Marinakis and Shergold, 1985;

Young and Miller, 2000). Three oleate adsorption mechanisms at the surface of salt-type minerals are proposed in the literature: (1) chemisorption that results from the direct interaction between oleate molecules and the Ca²⁺ ions exposed at the mineral surface; (2) surface precipitation whereby Ca²⁺ ions interact with the oleate molecules immediately after leaving the mineral lattice. The formed calcium oleate then precipitates at the mineral surface; and (3) bulk precipitation that assumes that interaction between Ca²⁺ ions and collector takes place in the solution bulk. The formed calcium oleate colloids can cover the mineral particles (heterocoagulation) depending on conditions that are governed by the DLVO theory (Finkelstein, 1989; Hanna and Somasundaran, 1976).

Lu et al. (1998) analyzed adsorption isotherms of oleate onto an apatite surface and compared their results with literature information about the adsorption of oleate on fluorite and calcite at pH 9.5. The authors observed that for oleate concentrations between 2×10^{-6} and 2×10^{-5} mol dm⁻³ the preferential adsorption order is: fluorite (surface calcium density = $1\overline{1.1}$ - $12.9 \,\mu\text{mol m}^{-2}$) > calcite (8.2 $\mu\text{mol m}^{-2}$) > apatite $(5.1-6.6 \, \mu mol \, m^{-2})$. This adsorption order is proportional to the calcium density at the mineral surface. On the other hand, for an oleate concentration greater than $2 \times 10^{-5} \text{ moldm}^{-3}$, the adsorption order changes to: calcite (solubility product $(K_{PS}) = 4.6 \times 10^{-9})$ > fluorite (5.0×10^{-11}) > apatite (6.3×10^{-126}) . This adsorption sequence is relative to the solubility product of minerals. These results indicate that surface precipitation takes place preferentially on the more soluble minerals (Lu et al., 1998). Nevertheless, the K_{PS} parameter is relative to an equilibrium condition, which probably does not take place during the flotation process. Therefore, it is necessary to study the dissolution kinetics of salt-type minerals in order to predict the behavior of these minerals in real systems.

Very few studies in the scope of mineral processing have been dedicated to investigate the influence of solubility/dissolution on flotation response of sparingly soluble minerals (Amankonah et al., 1985; Lu et al., 1998; Marinakis and Shergold, 1985). Marinakis and Shergold (1985) studied the effect of the presence of sodium oleate in the solubility of different salt-type minerals. It was observed that the dissolution of apatite, fluorite and calcite is inhibited by the oleate addition, probably due to the covering of the mineral surface by calcium oleate.

If different sparingly soluble minerals are present in solution, the dissolution of one phase can affect the dissolution of the others. According to Amankonah et al. (1985), although the apatite solubility is different from the calcite solubility in pure water, an intermediated value is reached as the reaction takes place in the supernatant of the other mineral. The found behavior was explained as a consequence of the formation of a third phase with characteristics of both calcite and apatite, and called "capatite" by the authors. Finkelstein (1989), however, suggested the formation of monetite (calcium hydrogenophosphate, CaHPO₄), whose solubility is less than that of calcite and greater than that of apatite.

Table 2 Characteristics of the apatite samples.

City of origin	Country	Genesis	Туре	Company	Identification
Araxá	Brazil	Igneous	Purified from ore	Vale	AAR
Cajati	Brazil	Igneous	Purified from ore	Vale	ACJ
Ipirá	Brazil	Igneous	Naturally pure	=	AIP
Santa Quitéria	Brazil	Metamorphic	Purified from ore	Brazilian Nuclear Industry (INB)	ASQ
Sra Ouertane	Tunisia	Sedimentary	Purified from ore	Groupe Chimique Tunisien	ASO

Dissolution kinetic of apatite has been investigated by works that are dedicated to the study of tissue and bone demineralization caused by diverse diseases (Papangkorn et al., 2008; Rootare et al., 1962). Some studies have approached the dissolution of natural apatites under relevant geological conditions (Dorozhkin, 1997a, 1997b; Guidry and Mackenzie, 2003; Valsami-Jones et al., 1998). In addition, there are investigations within the scope of industrial processing, such as fertilizer production (Chaïrat et al., 2007a, 2007b; Harouiya et al., 2007). In most of the works, dissolution is conducted in stirred reactors at a constant temperature. The reaction is followed by chemical analyses (Ca, P, F) of solution samples that are removed after different time periods (Chaïrat et al., 2007a, 2007b; Guidry and Mackenzie, 2003; Harouiya et al., 2007).

Several works have reported the reduction of the apatite dissolution rate as the pH increases until a transition region from which it is independent on pH (Chaïrat et al., 2007a, 2007b; Guidry and Mackenzie, 2003; Valsami-Jones et al., 1998). Guidry and Mackenzie (2003) found the transition region at pH 5–6 for fluorapatite and 4–7 for carbonate-fluorapatite. Chaïrat et al. (2007b) studied the dissolution of a fluorapatite from Brazil (Paraiba state) in the pH region from 2 to 12. The authors observed the dissolution rate reduction at pH 2 to 7 and 10 to 12. Between pH 7 and 10 dissolution was found to be independent of pH.

The apatite dissolution seems not to be stoichiometric in the early stages of reaction, in which Ca²⁺ ions are preferentially liberated. As dissolution evolves, however, the congruency can be reached (Chaïrat et al., 2007a, 2007b; Guidry and Mackenzie, 2003; Rootare et al., 1962). The incongruent dissolution might lead to the formation of intermediated phases on the apatite surface. These phases may be determined by the lattice composition of the apatite, as well as by the chemical composition of the dissolution medium (Chaïrat et al., 2007a; Rootare et al., 1962). Nevertheless, several works have reported that secondary phases are not formed and the intermediated phases can be modifications of the phosphate groups (Chaïrat et al., 2007a; Harouiya et al., 2007; Rootare et al., 1962).

Chaïrat et al. (2007b) analyzed the apatite dissolution by using Scanning Electron Microscopy (SEM). It was found that dissolution in acidic medium takes place by pit formation, while in basic medium surface modifications are not relevant. Dorozhkin (1997a) investigated two different levels of acidic dissolution of natural fluorapatite crystals: the millilevel, by using optical microscopy and the microlevel, by using SEM. At the millilevel the apatite dissolution was found to be determined by the dislocation structure of the crystals, resulting in permanent dissolution rate increases for the whole crystal. The microlevel dissolution process was found to have random irregularities, which appeared to be close to dimensions of the dislocated blocks.

The objective of this work was to investigate the relationship between dissolution kinetics and flotation response, with sodium oleate, of apatites from different genesis and origins. With the results it is intended to understand why different flotation strategies are applied to concentrate phosphate ores from different deposits (Igneous, sedimentary and metamorphic) around the world. Based on this knowledge it can be possible to improve the used flotation strategies, as well as to propose concentration approaches for new deposits.

2. Materials and methods

2.1. Apatite samples

Apatite samples from different origins and genesis (igneous, metamorphic and sedimentary) were firstly purified, and then submitted to characterization, dissolution and flotation experiments. The characteristics of the apatite samples, such as origin, genesis and identification are depicted in Table 2.

Most of the apatite samples (AAR, ACJ, ASO and ASQ) were purified from phosphate ores that are exploited by different mining groups (Table 2). The only exception is the apatite from Ipirá (AIP), which was handpicked in the reserve and presented adequate purity to be used in the experiments.

2.2. Purification of apatites

Purification of the apatite samples from phosphate ores was carried out by gravity concentration and magnetic separation. The first purification step was the removal of magnetic minerals by means of magnetic separation. The ore samples were firstly submitted to 6.0×10^{-2} T of magnetic field (Inbras, HFP RE-Ø15"×12 magnetic separator) in order to remove magnetite (Fe₃O₄) particles, then to 1.2×10^{-1} T (Inbras, RE-05/04-1 magnetic separator) to remove hematite (Fe₂O₃) and phlogopite (KMg₃(AlSi₃O₁₀)(F,OH)₂) particles.

Afterward, apatite (specific mass = $3.3 \, \mathrm{g \ cm^{-3}}$) was separated from carbonates (calcite, 2.71 g cm⁻³, and dolomite, 2.86–3.10 g cm⁻³) and silicates (2.6 g cm⁻³) by means of heavy media separation using bromoform (CHBr₃), whose specific mass is 2.98 g cm⁻³. Heavy media separation was also applied in order to remove heavier minerals such as barite (BaSO₄), whose specific mass is 4.3–4.6 g cm⁻³, by using diiodomethane (CH₂l₂) that has a specific mass of 3.32 g cm⁻³.

Each step of heavy media concentration was accomplished by centrifuging (FANEN, Excelsa II centrifuge) 1-5 g of ore with 25 cm³ of the adequate heavy liquid at 1500 rpm during 5 min. Next, the sink and float products were excessively washed with water and ethylic alcohol (C_2H_5OH), and dried at 40 °C.

The heavy media separation product, containing mainly apatite, was finally submitted to Frantz magnetic separation (Barreiro Frantz equipment) in a magnetic field of 0.6–1.5 T to remove composite particles. The used lateral and frontal inclinations in the Frantz equipment were 15° and 18°, respectively.

2.3. Characterization

The chemical composition of apatites was determined by X-Ray Fluorescence (XRF). The XRF analyses (Axios Advanced equipment, PANanalytical) were conducted with samples that were melted with anhydrous lithium tetraborate. The analyzed oxides were Na₂O, MgO, Al₂O₃, SiO₂, P₂O₅, SO₃, K₂O, CaO, TiO₂, MnO, Fe₂O₃ and SrO.

The Rietveld method applied to X-Ray Diffraction (XRD) data was used in order to quantify the content of apatite and impurities (calcite, dolomite, silicates and barite). The XRD data acquisition conditions (equipment Empyrean, PANanalytical) were: Cu radiation with wave length $(\gamma) = 1.54$ Å; Automatic divergence slit with irradiated area = 15 mm; Step = 0.013 and $2\Theta = 8$ to 140° .

Apatites were also submitted to heat loss (HL) analyses by calcination under 1050 °C during 1 h. This analysis yields the variation of mass after calcination which is related to the CO_3^{2-} content.

In addition, apatite samples were characterized by their physical properties: surface area (S), porosity (P) and specific mass. Surface area and porosity were determined by mercury porosimetry (Auto Pore IV, Micromeritics equipment). The specific mass was measured by helium picnometry (AccuPyc II 1340, Micromeritics equipment).

2.4. Dissolution experiments

Apatite dissolution experiments were carried out in an Atlas Potassium (Syrris) automated chemical reactor whose schematic representation is illustrated in Fig. 1. The equipment allows pH and temperature control and measurement, besides stirring control and the flow of the addition of one gas. The pH control is executed by adding acidic and basic solutions through two injection pumps. The control of temperature is accomplished by a thermostatic bath (Fanem) coupled to a temperature sensor. The dissolution is carried out in a 250 cm³ reactor in which the following components are introduced: temperature and pH sensors, capillaries for addition of acidic and basic solutions and a gas addition tube (Fig. 1). The reaction control is executed by means of the Atlas software.

The experiments were conducted in CO_2 -free solutions. Deletion of CO_2 was done by adding N_2 -gas into the reaction vessel 10 min before and during dissolution (Guidry and Mackenzie, 2003). N_2 addition for 10 min, before the experiments, was sufficient to stop the variation of the water pH. Ultrapure water (resistivity of 18.3 M Ω cm at 25 °C) was used in all experiments.

The dissolution experiments were carried out in three steps: (1) Firstly, the water temperature (150 cm³) was adjusted to 25 °C. (2) The water pH was adjusted to 8 or 10 by adding sodium hydroxide (NaOH) solutions at 0.005 and 0.010 mol dm³ respectively. Concurrently to the pH adjustment, N₂ was bubbled (100 \pm 0.1 cm³ min $^{-1}$) into the reaction vessel. (3) Finally, 1.5 g of apatite (particle size between 103 and 43 μ m) was introduced to the reaction vessel, and dissolution took place. Two dissolution experiments were conducted for each apatite sample.

The reaction was interrupted after different time periods (5, 10, 25 and 40 min), the solution was then filtered in a Millex HV filter (pores of 0.45 μ m and 33 mm in diameter). The filtered solutions (50.0 cm³) were acidified with two drops of concentrated nitric acid (H_2NO_3) and submitted to Ca^{2+} ions analysis by Inductively Coupled Plasma-Atomic Emission Spectrometry (ICP-AES).

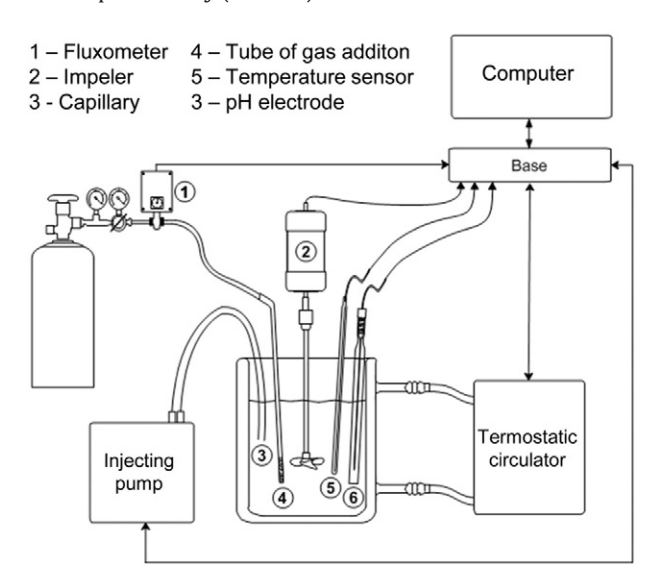


Fig. 1. Schematic representation of the Atlas potassium reactor.

The dissolution curves consist of the variation of accumulated amount of dissolved Ca²⁺ ions as a function of time (t). These curves were normalized by the apatite surface area in order to allow the comparison between apatite samples with different surface areas.

2.5. Flotation experiments

The flotation response of the apatite samples was determined by means of microflotation experiments with sodium oleate as collector, at pH 8 and 10. The sodium oleate concentration of 1.4×10^{-5} mol dm⁻³ was selected based on the premise that neither very high nor very low recoveries were convenient for the sake of comparing the flotation response of materials which exhibited different dissolution behaviors. The sodium oleate solutions were made with ultrapure water (R = 18.2 M Ω cm at 25 °C). The temperature of solutions was adjusted to 25 °C before any experiment by using a water bath. Microflotation was conducted in a modified Hallimond tube with 32.2 cm of diameter and 92.2 mm of height (Fig. 2). Agitation of 22.9 s⁻¹ was promoted by a mechanical stirring system coupled with a rotational speed controller. Three microflotation experiments were conducted with each apatite sample.

Flotation experiments were carried out by mixing 1.00 g of mineral (particle size between 103 μm and 43 μm) with 0.06 dm 3 of sodium oleate solution at the desired pH (8 or 10). After 1 min of conditioning, N_2 was introduced (0.8 cm 3 s $^{-1}$) in the system and flotation was accomplished within a length of time of 1 min. During flotation, the floated material was manually skimmed off the cell with a small ladle (Fig. 2). The yielded products (sink and float) were filtered, dried at 40 °C and weighed in order to determine the floatability (F).

3. Results

3.1. Characterization

The results of XRF analyses of the apatite samples are exhibited in Table 3. Stoichiometric fluorapatite displays 42.3% of P_2O_5 and a CaO/ P_2O_5 ratio equal to 1.31 (Klein and Dutrow, 2011). However, natural apatites may present different stoichiometry according to their genesis and geological history (Born et al., 1996; McClellan, 1980; Toledo et al., 2004; Toledo and Pereira, 2001). For the studied apatites, the P_2O_5 and CaO/ P_2O_5 content values varied between 35.5–42.3% and 1.31–1.49% respectively, as it is observed in Table 3.

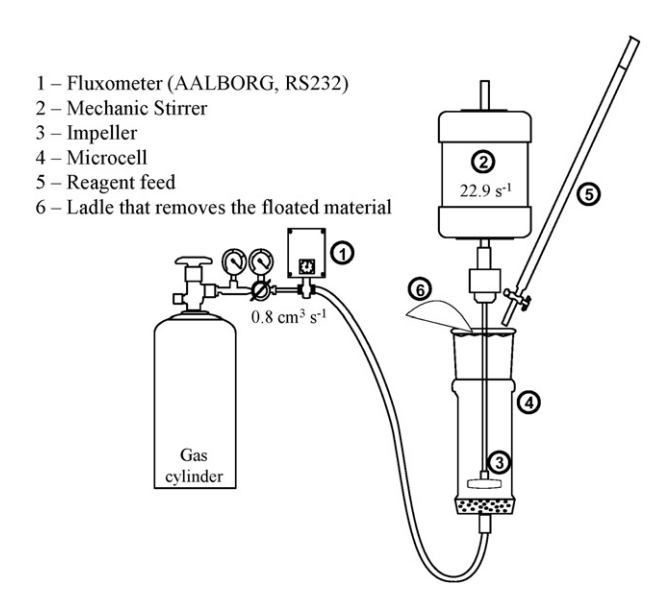


Fig. 2. Experimental apparatus of the microflotation experiments.

Table 3 XRF analyses of apatite samples.

Chemical species	AAR ^(b)	ACJ	AIP	ASQ	ASO
Na ₂ O	< 0.1	<0,1	< 0.1	0.6	0.6
MgO	0.1	< 0.1	< 0.1	0.1	0.4
Al_2O_3	< 0.1	< 0.1	<0,1	0.1	< 0.1
SiO ₂	0.5	< 0.1	1.6	2.1	0.9
P_2O_5	37.2	42.3	39.4	38.7	35.5
SO ₃	2.1	< 0.1	0.6	0.4	0.5
K ₂ O	< 0.1	< 0.1	< 0.1	< 0.1	< 0.1
CaO	50.8	55.4	54.4	52.6	52.9
TiO ₂	< 0.1	< 0.1	< 0.1	< 0.1	< 0.1
MnO	< 0.1	< 0.1	< 0.1	< 0.1	< 0.1
Fe_2O_3	0.4	< 0.1	< 0.1	3.2	0.2
SrO	0.9	0.4	< 0.1	0.3	0.2
LH ^(a)	1.2	0.3	0.6	1.9	7.4
CaO/P_2O_5	1.37	1.31	1.38	1.36	1.49

a HL = heating loss.

According to the XRF analysis the ACJ sample presents the least amount of impurities (only 0.4% of SrO) among the analyzed apatites. The AIP exhibits SiO₂ (1.6%) and SrO (0.4%) as the main impurities. The AAR stands out for its BaO content (3.7%) which indicates the presence of barite (BaSO₄). The ASQ sample contain SiO₂ (2.1%) and Fe₂O₃ (3.2%). The ASO apatite displays elevated LH that indicates the substitution of PO $_3^{4-}$ by CO $_3^{2-}$ ions in the apatite lattice, which is characteristic of carbonate-fluorapatite.

The mineralogical composition of the studied samples was identified by means of the semi-quantitative analysis by the Rietveld method (Table 4). With exception of the ACJ, a small amount of calcite was identified in all apatite samples. In agreement with the XRF results (Table 3), barite was found in the AAR apatite that presents the lowest purity (>97%). In addition, quartz was found in the AIP and ASQ apatites (Table 4), which is in agreement with their SiO_2 content of 1.6% and 2.1%, respectively (Table 3).

The found specific mass, surface area and porosity of apatite samples can be observed in Table 5. The apatites specific mass varies from 3.024 to 3.221 g cm $^{-3}$, obeying the following increasing order regarding their genesis: igneous > metamorphic > sedimentary (Table 5). These values are in agreement with the specific mass theoretical values for fluorapatite, which is 3.16–3.22 g cm $^{-3}$ (Klein and Dutrow, 2011). According to Toledo and Pereira (2001), differences in specific mass of the apatites are related to their variability of composition due to diverse possible lattice substitutions.

Although the particle size range is the same (43–103 µm) for all studied apatites, their surface area (S) varies to a large extent, as can be observed in Table 5. The surface area variation is related to differences in surface irregularities as well as surface porosity. The sedimentary apatite (ASO) exhibits a much larger surface area (S = 85,520 cm² g $^{-1}$) than the other samples (60 \leq S \leq 2710 cm² g $^{-1}$). The metamorphic sample (ASQ) presents an intermediate value of S (2710 cm² g $^{-1}$), while the igneous samples exhibit the lowest surface areas (<320 cm² g $^{-1}$).

Regarding porosity, the results in Table 5 reveal that the samples with higher porosity values also present larger surface areas. Therefore,

Table 4Results of the purity analysis by the Rietveld method.

Apatite	Mineralogical comp	Mineralogical composition		
Apatite	Apatite (%)	Impurities		
AAR	97	Barite, calcite and dolomite		
ACJ	>99	-		
AIP	99	Quartz and calcite		
ASQ	99	Quartz and calcite		
ASO	99	Calcite		

Table 5Physical properties of apatites.

Apatite	Specific mass (g cm ⁻³)	Surface area (cm² g ⁻¹)	Porosity (%)
AAR	3.221 ± 0.003	320	2.44
ACJ	3.205 ± 0.007	60	2.46
AIP	3.202 ± 0.004	60	2.12
ASO	3.024 ± 0.001	85,520	12.72
ASQ	3.139 ± 0.001	2710	4.82

the apatites ASO (S = 85,52 cm² g⁻¹; P = 12.72%) and ASQ (S = $2.71 \text{ cm}^2 \text{ g}^{-1}$; P = 4.82%) present the highest P and S values.

3.2. Dissolution

All dissolution curves (accumulated Ca²⁺ ions as a function of time) exhibited an exponential profile, which is in agreement with a first order reaction in relation to Ca²⁺ ions. Fig. 3 presents examples of dissolution curves for the AAR at pH 8 and 10.

The dissolution curves were adjusted to Eq. (2), which allowed the determination of the maximum amount of dissolved Ca^{2+} ions (Ca^{2+}_{MAX}) as well as the kinetics constant (k).

$$nCa^{2+} = Ca_{MAX}^{2+} (1 - e^{-kt}).$$
 (1)

The ${\sf Ca^{2+}}_{\sf MAX}$ parameter informs the amount of ${\sf Ca^{2+}}$ ions dissolved after the reaction reaches the steady state, which corresponds to the dissolution curve plateau (Fig. 3). The kinetic constant expresses how fast the steady state is reached. In addition, the initial rate of dissolution (R_i) was calculated by adjusting the first minutes of dissolution to a straight line. The relevancy of this parameter is based on the fact that it represents the time period of the microflotation experiments (1 min of conditioning and 1 min of flotation).

The apatite samples from different origins presented different behavior in the dissolution experiments as can be observed in the bar diagram of Fig. 4 which contains the values of $R_{\rm i}$, $\text{Ca}^{2+}_{\text{MAX}}$ and k. The values of $R_{\rm i}$ and $\text{Ca}^{2+}_{\text{MAX}}$ are greater at pH 8 than at pH 10, which indicates that at pH 8 dissolution is faster and provides more Ca^{2+} ions to solution at the steady state (Fig. 4). The reduction of apatite dissolution rate as the pH increases was reported by Guidry and Mackenzie (2003) for pH 2 to 8. On the other hand, Chaïrat et al. (2007b) reported no dissolution rate variation between pH 7 and 10.

The initial dissolution rate (R_1) of apatites from different origins follows the decreasing order ACJ > AIP > ASQ > AAR > ASO, regardless of the reaction pH. With exception of the AIP at pH 8, the Ca²⁺_{MAX} parameter

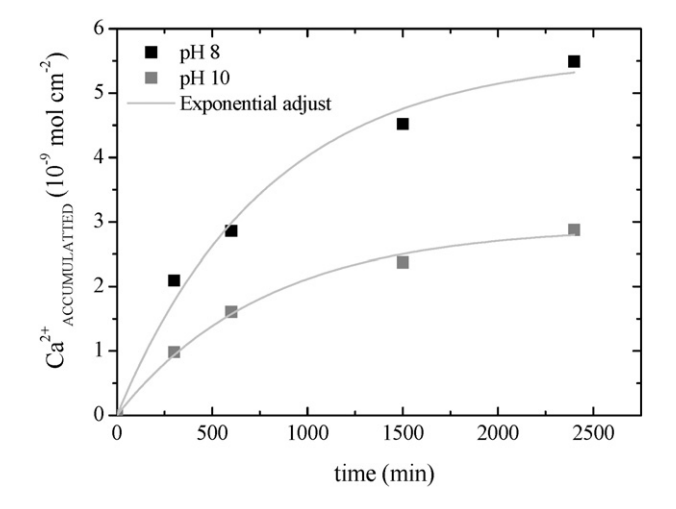


Fig. 3. Dissolution curve (accumulated Ca²⁺ ions as a function of time) for the AAR apatite.

b AAR contains 3.7% of BaO.

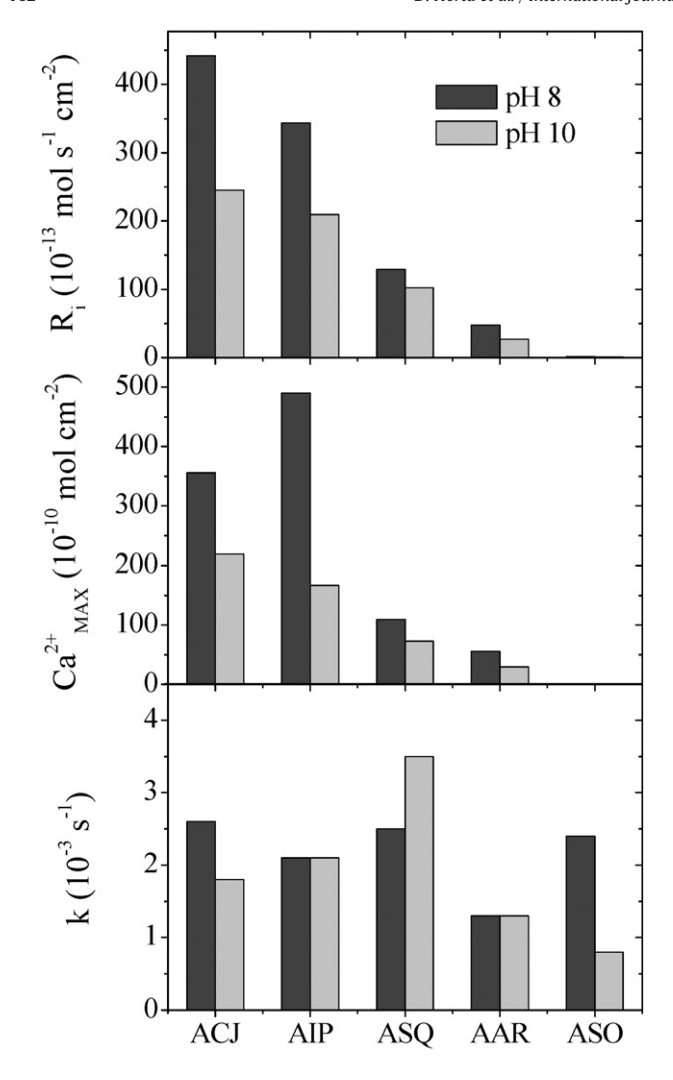


Fig. 4. Parameters of apatite dissolution: initial rate (R_i) , maximum amount of dissolved Ca^{2+} ions (Ca^{2+}_{MAX}) and kinetic constant (k).

follows the same decreasing sequence found for R_i (Fig. 4). Therefore, apatites that dissolve faster in the initial stages of reaction, give more ${\rm Ca^2}^+_{\rm MAX}$ ions to solution after the steady state is reached.

Regarding the kinetic constant, it seems not to present the same tendency found for R_i and ${\rm Ca^2}^+{}_{\rm MAX}$ (Fig. 4). Thus, the rate with which the steady state is reached seems not to depend on the origin of the sample nor the pH of reaction.

3.3. Flotation response

Results of floatability are compared by means of a bar diagram in Fig. 5. It can be observed that, independent of the origin, floatability at pH 8 is greater than at pH 10. This result indicates that the floatability of each apatite is higher in the condition that provides the greater initial dissolution rate (pH 8 in instead of pH 10).

Comparing the apatites, the decreasing order of floatability is: $ACJ - AIP \gg AAR > ASQ > ASO$ (Fig. 5).

3.4. Discussion

According to the microflotation results (Fig. 5), the increasing flotation performance of apatites can be expressed in terms of the genesis as: igneous > metamorphic > sedimentary. This order of flotation response with sodium oleate is in agreement with the results of Rodrigues and

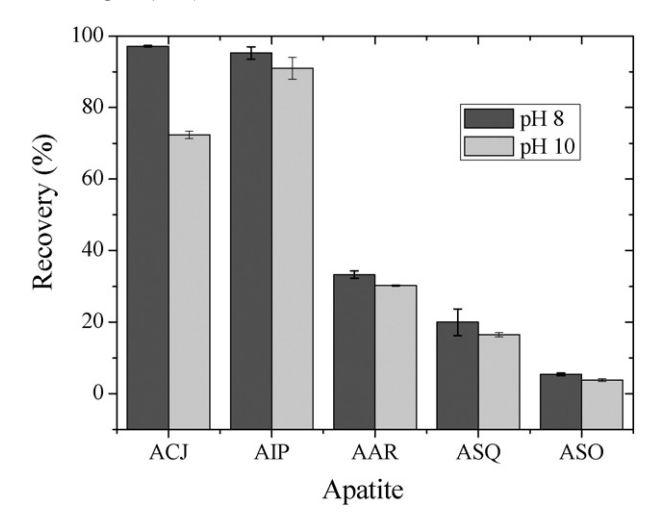


Fig. 5. Flotation response of a patite using sodium oleate as collector $(1.4 \times 10^{-5} \ {\rm mol} \ {\rm dm}^{-3}).$

Brandão (1993) who reported that igneous apatite presents greater floatability than sedimentary samples.

Considering that the concentration of collector was kept constant, this result means that in order to achieve the flotation performance of the igneous apatite, it is necessary to increase the collector dosage for sedimentary and metamorphic samples. This result is in agreement with the surface area since this parameter increases according to the genesis as: igneous > metamorphic > sedimentary. With the increase in the surface area the necessity use of a higher concentration of collector is expected in order to promote the adequate hydrophobicity for flotation. This information is supported by the Fig. 6 that shows the correlation between flotation recovery and surface area. Regardless of the pH the flotation recovery decreases as the surface area increases. With the increased of surface area, an extra amount of collector is required for an effective recovery.

Regarding the pH influence, as observed in Fig. 5, the floatability of apatite is greater at pH 8 than at pH 10. This outcome follows the initial dissolution rate (R_i) , that is also greater at pH 8 than at pH 10. As such, the results indicate that the faster the apatite dissolution, the greater its floatability.

The influence of dissolution on flotation response of apatites from different origins was analyzed by means of linear associations between floatability and dissolution parameters (Fig. 7). The apatite floatability (F) increases with R_i at pH 8 (R =0.95) and pH 10 (R =0.89), which again indicates the apatites which dissolve quicker, exhibit higher

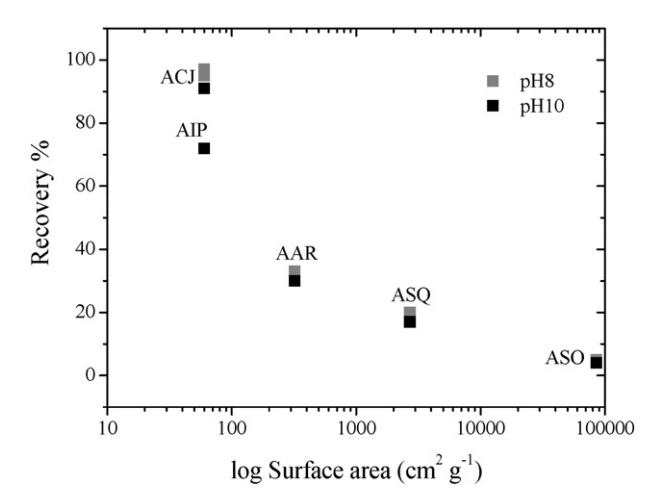


Fig. 6. Flotation recovery as a function of surface area.

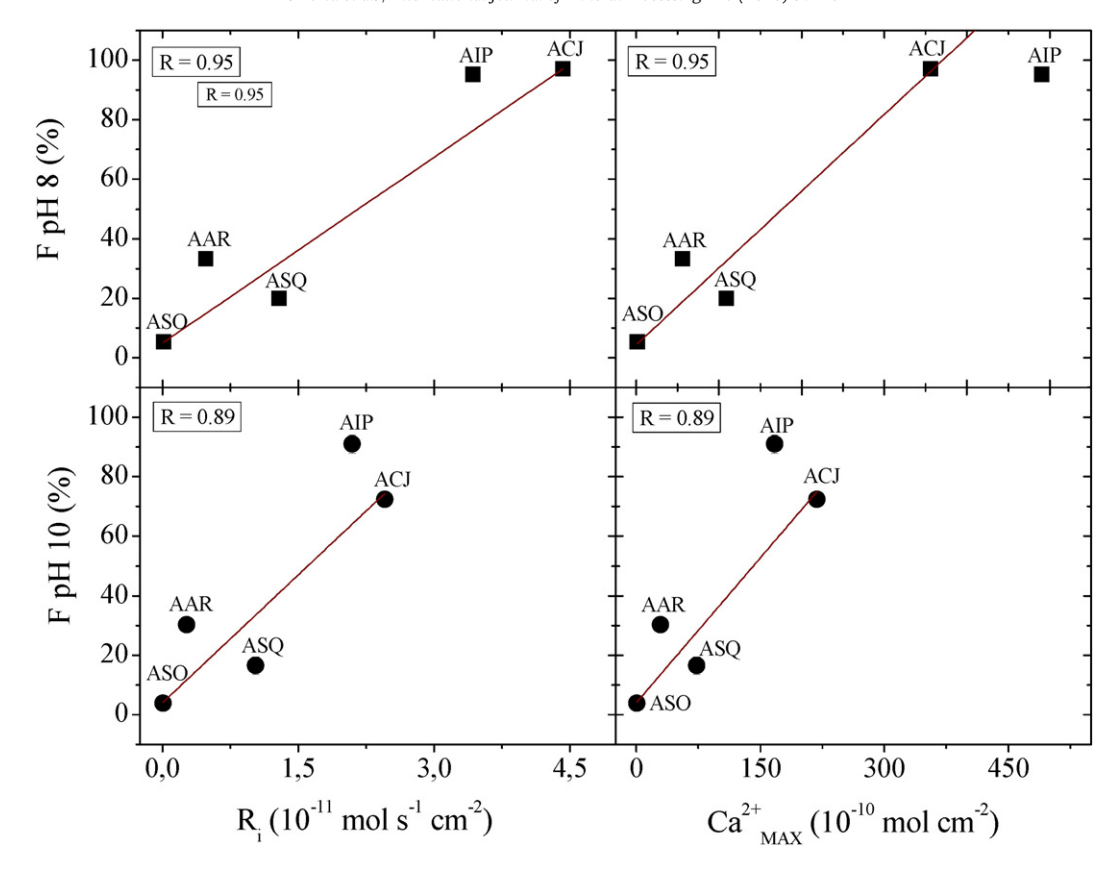


Fig. 7. Floatability (F) as a function of the dissolution parameters R₁ (initial rate) and Ca²⁺_{MAX} (maximum amount of dissolved calcium ions) at pH 8 and 10.

flotation performance. Floatability also enhances as ${\rm Ca^{2+}}_{\rm MAX}$ increases at pH 8 (R = 0.95) and pH 10 (R = 0.89), suggesting that the higher the maximum amount of ${\rm Ca^{2+}}$ ions dissolved, the higher the floatability. Nevertheless, k seems do not be related with apatite floatability since the correlation coefficients display low values: R = 0.16 at pH 8 and R = -0.36 at pH 10.

The linear relationship between floatability and initial dissolution rate at pH 8 and 10 is presented in Eqs. (3) and (4), respectively.

$$pH8: F = 8.9 + 21.5R_i (10^{-11})$$
 (2)

(R = 0.95)

$$pH\ 10: F = 7.1 + 30, 5R_i \Big(10^{-11}\Big) \eqno(3)$$

(R = 0.89).

The constants of Eqs. (3) and (4) (21.5 for pH 8 and 30.5 for pH 10) display similar values (same order of magnitude), that indicates that the pH could be introduced to the model. It requires the conduction of other dissolution and flotation experiments using different pH values.

In summary, a variation of apatite floatability and dissolution with pH (8 or 10) and a relationship between floatability and dissolution for the different apatites was observed. These results might be discussed in terms of the suitable condition of calcium oleate ((RCOO)₂Ca) formation according to the reaction 4 (Finkelstein, 1989).

$$2RCOO^{-} + Ca^{2+} = (RCOO)_{2}Ca$$
 (4)

in which R is the polar chain of the oleate $(CH_3(CH_2)_{14}(CH)_2)$ that presents one double bond at the carbon 9. According to Du Rietz (1975) the solubility product of calcium oleate is 3.98×10^{-16} .

According to the surface precipitation mechanism, calcium oleate is formed by means of the reaction expressed in Eq. (4) after interaction between Ca²⁺ dissolved ions and the collector oleate (RCOO⁻) near the apatite surface, and then precipitates at the surface. The covering of apatite particles by the calcium oleate is responsible for the introduction of hydrophobicity and consequent flotation (Hanna and Somasundaran, 1976; Finkelstein, 1989; Lu et al., 1998; Young and Miller, 2000).

The influence of R_i on the flotation response with sodium oleate of apatites from different origins at pH 8 and 10 elucidates the relevance of the surface precipitation mechanism governing the adsorption of oleate at the apatite surface. The apatites that dissolve quickly make more Ca^{2+} ions available to interact with oleate molecules and form calcium oleate, which precipitates on the apatite surface promoting hydrophobicity.

Taking the example of ACJ, the initial dissolution rate is much higher at pH 8 (442.4 \times 10^{-13} mol s $^{-1}$ cm $^{-2}$) than at pH 10 (245.4 \times 10^{-13} mol s $^{-1}$ cm $^{-2}$). Therefore, after 1 min of being in contact with the aqueous medium, more Ca $^{2+}$ ions are provided for solution at pH 8 (3.2 \times 10^{-7} mol dm $^{-3}$) than at pH 10 (1.33 \times 10^{-7} mol dm $^{-3}$). Being such, the formation of calcium oleate can be thermodynamically more favorable at pH 8 because the product [Ca $^{2+}$]x[oleate ion] 2 is higher at this condition.

The found relationship between floatability and dissolution supports the different flotation response of ores from different origins and genesis, which results in the dissimilar strategies of concentration observed in Table 1. In this context, the determination of the dissolution rate of apatite could be used as a characterization role in order to predict the flotation behavior of ores, as well as the necessary dosage of collector.

4. Conclusions

In terms of the genesis, the increasing floatability order found was: igneous > metamorphic > sedimentary. This result is in agreement

with the surface area values. For the same level of collector concentration, the floatability decreased with the surface area. Therefore, the floatation of sedimentary and metamorphic apatites must be conducted with higher collector dosage in order to reach the same floatation performance of the igneous samples.

The flotation performance of apatite was found to be greater at pH 8 than at pH 10. This result is explained by the fact that this mineral dissolves faster at pH 8 compared with pH 10.

By correlating apatites from different origins and genesis it was observed that the samples that presented greater initial dissolution rate values and provided more Ca^{2+} ions to solution at the steady state presented higher floatability. This result also indicates that apatites that provide more Ca^{2+} ions to interact with oleate molecules presented greater flotation performance.

The results emphasize the achievement of the surface precipitation mechanism on adsorption of oleate at the apatite surface during flotation. According to this mechanism, calcium oleate is formed after dissolution of Ca²⁺ ions, and then precipitates at the apatite surface promoting hydrophobicity. Accordingly, the flotation performance is expected to be improved by the increase of available Ca²⁺ ions in solution. This agrees with the observed results that apatite floatability increases with the rise of the initial dissolution rate and consequent increase of available Ca²⁺ ions.

Acknowledgments

The authors are grateful to Vale Mining Company that financially supported this research by means of the AMIRA P260F project. We are also grateful to Pananalytical Laboratory in which the X-Ray Diffraction analyses were accomplished and Professor Carlos O. Paiva-Santos and Dr.^a Selma Gutierrez Antonio who assisted with the Rietveld analyses.

References

- Abdel-Khalek, N.S.A., 2000. Evaluation of flotation strategies for sedimentary phosphates with siliceous and carbonates gangues. Miner. Eng. 13, 789–793.
- Abouzeid, A.Z.M., 2008. Physical and thermal treatment of phosphate ores an overview. Int. J. Miner. Process. 85, 59–84.
- Abouzeid, A.Z.M., El-Jallad, I.S., Orphy, M.K., 1980. Calcareous phosphates and their calcined products. Miner. Sci. Eng. 12, 73–83.
- Amankonah, J.O., Somasundaran, P., Ananthapadmanabhan, K.P., 1985. Effects of dissolved mineral species on the dissolution/precipitation characteristics of calcite and apatite. Colloids Surf. 15, 295–307.
- Assis, S.M., Maia, G.S., Coelho, E.M., Silva, J.M., 1985. Contribuição à interpretação das características de flutuabilidade do sistema calcita/apatita. Proceedings of the National Meeting of Mineral Processing and Extractive Metallurgy, 20-24th November, Natal, pp. 87–101.
- Assis, S.M., Viana, S.M., Silva, J.M., 1987. Calcitas, dolomitas e apatitas. Algumas características inerentes X microflotação. Proceedings of the National Meeting of Mineral Processing and Extractive Metallurgy, 18-22th October, Rio de Janeiro, pp. 265–280.
- Born, H., Lenharo, S.L.R., Kahn, H., 1996. Mineralogical characterization of apatites from Brazilian phosphate deposits. Trans. Inst. Min. Metall., Sect. B 1001, 117–126.
- Chaïrat, C., Oelkers, E.H., Schott, J., Lartigue, J.E., 2007a. Fluorapatite surface composition in aqueous solution deduced from potentiometric, electrokinetic, and solubility measurements, and spectroscopic observations. Geochim. Cosmochim. Acta 71, 5888–5900.
- Chaïrat, C., Schott, J., Oelkers, E.H., Lartigue, J.E., Harouiya, N., 2007b. Kinetics and mechanism of natural fluorapatite dissolution at 25 °C and pH from 3 to 12. Geochim. Cosmochim. Acta 71, 5901–5912.
- Dorozhkin, S.V., 1997a. Acidic dissolution mechanism of natural fluorapatite I. Mili and microlevels of investigation. J. Cryst. Growth 182, 125–132.

- Dorozhkin, S.V., 1997b. Acidic dissolution mechanism of natural fluorapatite II. Nanolevel of investigation. J. Cryst. Growth 182, 133–140.
- Du Rietz, C., 1975. Chemisorption of collectors in flotation. Proceedings of the International Mineral Processing Congress, 20–26th April, Cagliari, Instituto di Arte Mineraria, pp. 27–29.
- Finkelstein, N.P., 1989. Review of the interactions in flotation of sparingly soluble calcium minerals with anionic collectors. Trans. Inst. Min. Metall. Sect. C 988, 157–178.
- Guidry, M.W., Mackenzie, F.T., 2003. Experimental study of igneous and sedimentary apatite dissolution: control of pH, distance from equilibrium, and temperatures on dissolution rates. Geochim. Cosmochim. Acta 67, 2249–2963.
- Hanna, H.S., Somasundaran, P., 1976. Flotation of salt-type minerals. Fuerstenau, M.C. Flotation: Gaudin Memorial Volume. American Institute of Mining, Metallurgical, and Petroleum Engineers, New York, pp. 197–272.
- Harouiya, N., Chaïrat, C., Köhler, J., Gout, R., Oelkers, E.H., 2007. The dissolution kinetics and apparent solubility of natural apatite in closed reactors at temperatures from 5 to 50 °C and pH from 1 to 6. Chem. Geol. 244, 554–568.
- Horta, D.G., 2013. Efeito da Cristalinidade e da Cinética de Dissolução no Desempenho da Flotação de Apatitas e Calcitas PhD diss. University of Sao Paulo.
- Klein, C., Dutrow, B., 2011. Mineral Science. 23rd ed. Jay O'Callaghan, United States of
- Lawendy, T.A.B., McClellan, G.H., 1993. Flotation of dolomitic and calcareous phosphate ores. In: El-Shall, H., Moudgil, B.M., Wiegel, R. (Eds.), Beneficiation of Phosphates: Theory and Practice. Society of Mining, Metallurgy, and Exploration, Littleton, pp. 29–43.
- Leal Filho, L.S., 1991. Aspectos relevantes na separação apatita/minerais de ganga via processo Serrana PhD diss. University of Sao Paulo.
- Leal Filho, L.S., Martins, M., Horta, D.G., 2010. Concentration of igneous phosphate ores via froth flotation: challenges and developments. Proceedings of the International Mineral Processing Congress, 6–10th September, Brisbane, pp. 3–13.
- Lu, Y., Drelich, J., Miller, D., 1998. Oleate adsorption at an apatite surface studied by ex-situ FTIR internal reflection spectroscopy. J. Colloid Interface Sci. 202, 462–476.
- Marinakis, K.I., Shergold, H.L., 1985. The mechanism of adsorption in the presence of fluorite, calcite and barite. Int. J. Miner. Process. 14, 161–176.
- McClellan, G.H., 1980. Mineralogy of carbonate fluorapatites. J. Geol. Soc. 137, 675–681. Papangkorn, K., Yan, G., Heslop, D.D., Moribe, K., Baig, A.A., Otsuka, M., Higuchi, W.I., 2008. Influence of crystallite microstrain on surface complexes governing the metastable equilibrium solubility behavior of carbonated apatites. J. Colloid Interface Sci. 320,
- Pugh, R., Stenius, P., 1985. Solution chemistry studies and flotation behavious of apatite, calcite and fluorite minerals with sodium oleate collector. Int. J. Miner. Process. 15, 193–218.
- Rodrigues, A.J., Brandão, P.R.G., 1993. The influence of crystal chemistry properties on the floatability of apatites with sodium oleate. Miner. Eng. 6, 643–653.
- Rootare, H.M., Deitz, V.R., Carpenter, F.G., 1962. Solubility product phenomena in hydroxyapatite water systems. J. Colloid Sci. 17, 179–206.
- Silva, J.M., Leal Filho, L.S., Coelho, E.M., Assis S.M., 1985. Continuação de apatitas brasileiras e hidrofobicidade na presença de oleato de sódio. In: In: Proceedings of the National Meeting of Mineral Processing and Extractive Metallurgy, 20-24th November, Natal, pp. 87–101
- Sis, H., Chander, S., 2003a. Reagents used in the flotation of phosphate ores: a critical review. Miner. Eng. 16, 577–585.
- Sis, H., Chander, S., 2003b. Improving froth characteristics and flotation recovery of phosphate ores with nonionic surfactants. Miner. Eng. 16, 587–595.
- Snow, R., Zhang, P., 2006. Challenging the Crago "double float" process IV: selectivity enhancement in all-anionic flotation of Florida phosphates. In: Zhang, P., Miller, J., El-Shall, H. (Eds.), Beneficiation of Phosphates: Technology and Sustainability. The Society of Mining, Metallurgy, and Exploration, Florida, pp. 113–122.
- Toledo, M.C.M., Pereira, V.P.A., 2001. Variabilidade de composição da apatita associada a carbonatitos. Rev. Inst. Geol. 22, 27–64.
- Toledo, M.C.M., Lenharo, S.L.R., Ferrari, V.C., Fontan, F., Parseval, P., Leroy, G., 2004. The compositional evolution of apatite in the weathering profile of the catalão I alkaline-carbonatitic complex, goias, Brazil. Can. Mineral. 42, 1139–1158.
- Valsami-Jones, E., Ragnarsdottir, K.V., Putnis, A., Bosbach, D., Kemp, A.J., Cressey, G., 1998. The dissolution of apatite in de presence of aqueous metal cations at pH 2–7. Chem. Geol. 151, 215–233.
- Yehia, A., Miller, J.D., Ateya, B.T., 1993. Analysis of the adsorption behavior of oleate on some synthetic apatites. Miner. Eng. 6, 79–86.
- Young, C.A., Miller, J.D., 2000. Effect of temperature on oleate adsorption at a calcite surface: an FT-NIR/IRS study and review. Int. J. Miner. Process. 58, 331–350.
- Zheng, S., Cao, X., Ge, Z., Song, W., 2006. Beneficiation studies on sedimentary siliceous and calcareous phosphate ores in China. In: Zhang, P., Miller, J., El-Shall, H., Stana, R. (Eds.), Beneficiation of Phosphates IV: Technology and Sustainability. The Society of Mining, Metallurgy, and Exploration, Florida, pp. 217–221.